Terahertz dynamics of spins and charges in $CoFe/Al_2O_3$ multilayers

J. D. Costa,[1,*] T. J. Huisman,[2] R. V. Mikhaylovskiy,[2] I. Razdolski,[2] J. Ventura,[1,†] J. M. Teixeira,[1] D. S. Schmool,[1,3] G. N. Kakazei,[1] S. Cardoso,[4] P. P. Freitas,[4] Th. Rasing,[2] and A. V. Kimel[2]

[1]*IFIMUP and IN-Institute of Nanoscience and Nanotechnology, and Departamento de Fisica, Faculdade de Ciencias, Universidade do Porto, Rua do Campo Alegre, 687, 4169-007, Porto, Portugal*

[2]*Radboud University Nijmegen, Institute for Molecules and Materials, Heyendaalseweg 135, 6525, Nijmegen, The Netherlands*

[3]*Laboratoire PROMES CNRS (UPR 8521), Universitè de Perpignan Via Domitia, Rambla de la Termodynamique, Tecnosud, 66100, Perpignan, France*

[4]*INESC-MN and IN-Institute of Nanoscience and Nanotechnology, Rua Alves Redol, 9-1, 1000-029, Lisbon, Portugal*

(Received 1 August 2014; revised manuscript received 27 February 2015; published 12 March 2015)

The ultrafast laser-induced response of spins and charges in $CoFe/Al_2O_3$ multilayers are studied using THz and optical pump-probe spectroscopies. We demonstrate the possibility of ultrafast manipulation of the transport and magnetic properties of the multilayers with femtosecond laser excitation. In particular, using time-resolved THz transmission experiments we found that such an excitation leads to a rapid increase of the THz transmission (i.e., electric resistivity). Our experiments also reveal that femtosecond laser excitation results in the emission of broadband THz radiation. To reveal the origin of the emitted THz radiation, we performed magnetic-dependent measurements of the THz emission. We also compared the observed electric field of the THz radiation to calculations performed using subpicosecond laser-induced demagnetization measurements. The good agreement between the experimentally obtained spectra and the calculations corroborates that the measured THz emission originates from the demagnetization process.

DOI: 10.1103/PhysRevB.91.104407 PACS number(s): 42.25.Ja, 75.78.Jp, 78.20.Ls, 78.47.−p

The demand for ever faster and energy efficient data processing has continuously fueled fundamental research on magnetism over the last decades and resulted in the emergence and the rapid development of spintronic technology [1]. At the same time, the engineering of spintronic devices operating at THz frequencies remains a major challenge that could be met by the optical manipulation of spins at subpicosecond time scales.

One of the most efficient ways to study the ultrafast dynamics of magnetic materials and structures is based on the pump-probe technique, in which ultrashort optical laser pulses are used to induce and probe magnetization dynamics [2]. With the help of pump-probe techniques many exciting phenomena have been demonstrated, such as ultrafast demagnetization [3], coherent manipulation of spins with the help of circularly polarized light [4], or helicity dependent all-optical magnetic switching [5].

At the same time, THz time domain spectroscopy (TDS) [6] is a technique that has been broadly used to characterize material properties in the THz spectral region. In fact, since this frequency range corresponds to the characteristic energy of electronic intraband transitions [7], it allows the probing of charge carrier dynamics. There are several known examples of these kinds of studies for bulk semiconductors and semiconductor nanostructures [8–13]. Moreover, THz-TDS can be used to investigate magnetic phenomena, like ultrafast demagnetization [14,15], precessional modes of magnetic sublattices [16–19], as well as novel phenomena [20].

Despite the amount of reports on either ultrafast spin dynamics or THz-TDS, the combined investigation of the dynamics of spins and charges in technologically relevant materials is still scarce [21]. The conjugation of both measurements in materials that depict magnetoresistance may elucidate the role of the electrical and magnetic counterpart in transport phenomena and even push spintronics to the THz region. Here, we study how charges (i.e., free electrons) and spins respond to ultrafast stimuli such as an electric field at THz frequencies or a femtosecond laser pulse in $CoFe/Al_2O_3$ multilayers. These nanometric layers are widely used in the fabrication of spintronic devices, such as magnetic tunnel junctions [22,23].

A $[Co_{80}Fe_{20}$ (1.8 nm)$/Al_2O_3$ (3 nm)$]_{\times 10}$ multilayer was prepared by ion beam sputtering on 0.7-mm-thick glass substrates in a Nordiko 3000 tool and its static magnetic and electrical properties were reported previously [24–26]. The THz spectrometer used for the measurements was based on a Ti:sapphire regenerative amplifier which generates 50-fs laser pulses at the central wavelength of 800 nm with a repetition rate of 1 kHz and a pump fluence of 1 mJ/cm^2. A schematic representation of the THz-TDS setup is shown in Fig. 1. Two different configurations were used with very few modifications: one for THz transmission measurements (shutter open) and another for THz emission measurements (shutter closed). The red line represents the optical beam and the yellow the THz field. Small holes in the parabolic mirrors allow the optical beam to pass without significant loss of the THz field. The optical laser is divided in three branches: one for detection (1), one for THz generation (2), and one for optical pump excitation of the sample (3). For the measurements we employed an electrooptical detector, which allows us to determine the THz electric field. The electrooptical linear effect generates birefringence in materials with inversion symmetry upon the application of an electric field. In this case, the THz radiation induces the birefringence causing the rotation of the optical probe polarization. The THz signal is thus measured by resolving the polarization

*diogo.costa@visitor.inl.int
†joventur@fc.up.pt

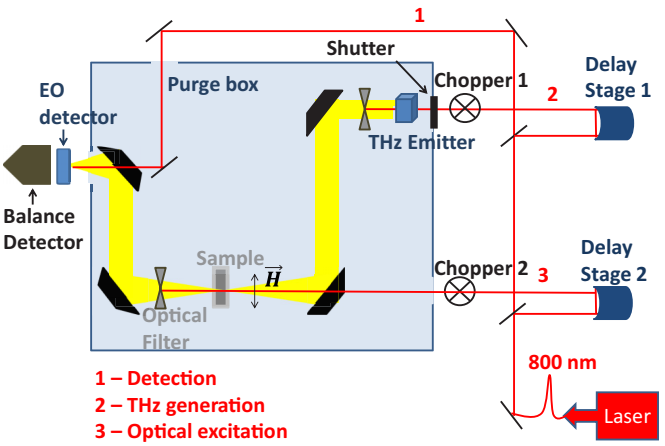

FIG. 1. (Color online) Schematic representation of the THz-TDS setup. The inset shows how each optical beam is used (1: detection, 2: THz generation, and 3: optical excitation).

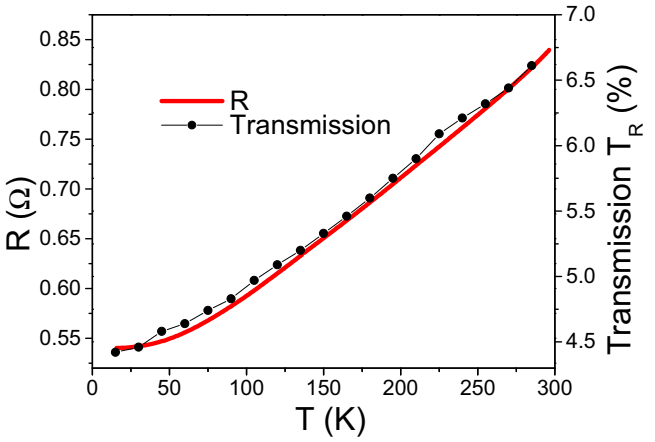

FIG. 2. (Color online) THz transmission (T_R) and resistance (R) as a function of temperature. The black dots represent the THz transmission normalized to the transmission of the substrate and the red line the resistance behavior for the same sample as reported elsewhere [24].

of the optical probe [27]. In the transmission measurements a THz emitter (a ZnTe crystal) is excited generating THz radiation. This radiation is focused on the sample and one can study how the THz transmission of the sample changes as a function of the optical pump delay time. In the case of the THz emission measurements the optical beam that would lead to the THz radiation of the ZnTe crystal is blocked and one can study the THz emission of the sample itself. The optical pump was focused onto the sample at normal incidence. The THz waves emitted from the optically pumped sample were measured after propagating through the glass substrate of the sample. An optical filter (transparent to THz radiation) was used to block the optical pulses. The purge box that involves the measurement setup was used to avoid the presence of water molecules that may absorb some of the THz radiation (N_2 was injected in the box). A cryostat was used to change the temperature sample from 300 to 15 K; the cryostat was only used in the temperature-dependent measurements, the remaining experiments were performed at room temperature. A schematic representation of the magnetic field direction applied during the measurements is also shown in Fig. 1.

To probe the ultrafast magnetization dynamics, a time-resolved stroboscopic magnetooptical pump-probe technique was employed. A Ti:sapphire laser system in combination with an amplifier was used to generate laser pulses similar to the optical pump used in the THz measurements with a repetition rate of 250 kHz (and the same pump fluence of 1 mJ/cm^2). The same pulse was used as the optical probe, but with a beam intensity at least 100 times lower.

With the aim of understanding to what extent THz transmission measurements can serve as a probe of transport properties in CoFe/Al_2O_3 multilayers at THz frequencies, we measured the THz transmission through the multilayer structure as a function of temperature T. To deduce the signal originating from the CoFe/Al_2O_3 multilayer, we normalized the electric field transmission of the sample with that of the substrate. The result is shown in Fig. 2 (black dots). One sees that the THz transmission through the CoFe/Al_2O_3 multilayer increases with temperature. This can be understood if one assumes that the transmission is dominated by the real part of the electric conductivity. As the temperature decreases, the scattering rate of free electrons becomes smaller, thereby leading to an increase of the conductivity and thus a decrease of the transmission of the electromagnetic radiation at THz frequencies. There is a remarkable correlation between the temperature dependencies of the THz transmission with the d.c. electrical resistance, see Fig. 2. This finding confirms that the THz transmission can serve as a probe of the transport properties of spintronics materials at THz frequencies.

To understand if it is possible to control the transport properties of the multilayer structure with the aid of a femtosecond laser pulse, we have performed time-resolved pump-probe measurements in which the sample was first excited by a 50-fs laser pulse and the laser-induced changes were probed with a pulse of THz radiation. Varying the delay between the pump and probe pulses we measured how the maximum electric field of the transmitted THz pulse changes as a function of the delay. The results are shown in Fig. 3(a), where the change in the transmission is measured with respect to the transmission without pump pulses present. It is seen that the femtosecond laser excitation can indeed cause ultrafast dynamics of the THz transmission. In particular, the time-resolved measurements reveal three different regimes of the dynamics: the steep change of the THz transmission on a time scale of $\sim$ 500 fs, a fast decay on a time scale of 0.8 ps and a slower relaxation with the characteristic time of about 140 ps. The dynamics can be understood using the two-temperature model, which describes the temporal evolution of the system in terms of two coupled reservoirs of energy representing free electrons and lattice, respectively [28],

$$C_e(T_e)\frac{dT_e}{dt} = -G(T_e - T_l) + P(t), \quad (1)$$

$$C_l(T_l)\frac{dT_l}{dt} = G(T_e - T_l), \quad (2)$$

where C_l and C_e are heat capacities of the lattice and the electrons, respectively. T_l is the lattice temperature, T_e is the

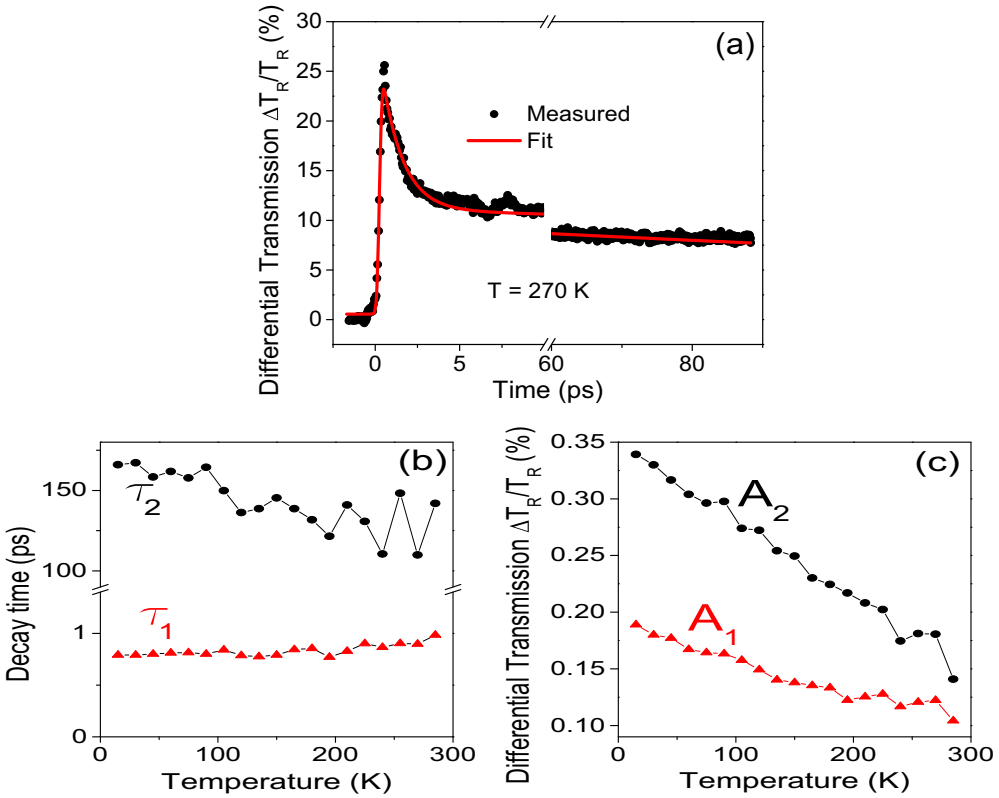

FIG. 3. (Color online) Change in THz peak transmission after an incident optical pump pulse. (a) The change in THz transmission (relatively to the transmission without the pump pulse $\Delta T_R/T_R$) can be fitted with Eq. (3). (b) Characteristic times and (c) amplitude of the decays of the photo-induced transmission change during the fast recovery (τ_1) and the slow cooling rate (τ_2).

temperature of the electrons, G the electron-lattice coupling factor, and $P(t)$ the laser heating source. When an intense 50-fs laser pulse is absorbed in the medium, its energy is transferred to the electron gas, increasing its temperature/energy. This leads to an increase of the scattering rate and results in a decrease of the conductivity. As a result, the THz transmission increases and, as can be seen from the experiment in the studied materials, this increase occurs faster than 0.5 ps ($\tau_0 < 0.5$ ps). From the differential equations it is seen that the time scale of the process is defined by the time dependence of the source $P(t)$. After that, due to electron-phonon coupling, the electrons will effectively transfer their energy to the lattice on a time scale below 1 ps [29,30] ($\tau_1 \sim 0.8$ ps). Phenomenologically, we were able to describe the transmission change due to a pump pulse using

$$\frac{\Delta T_R}{T_R} = \left[0.5\mathrm{erf}\left(\frac{t}{\tau_0} - 0.5\right)\right]\left[A_1\exp\left(-\frac{t}{\tau_1}\right) + A_2\exp\left(-\frac{t}{\tau_2}\right)\right], \quad (3)$$

where τ_0 is the rise time of the error function, A_1 and A_2 are exponential amplitudes, and τ_1 and τ_2 are exponential decay times. The first term between brackets in Eq. (3) describes the sudden change in the resistivity, while the exponential decays account for the different relaxation processes. The function described in Eq. (3) can perfectly describe our photoinduced transmission change, as shown with the solid line in Fig. 3(a). The decay time τ_1 can be interpreted as the characteristic time of the electron-phonon coupling the strength of which is described by the factor G [see Eqs. (1) and (2)]. The observed decrease of the THz transmission originates from an increase of the THz conductivity and indicates that this electron-lattice thermalization leads to a temperature decrease of the system. One should point out that the resistance of a metal is governed by both electron-electron and electron-phonon scattering. It is expected that the electron-electron scattering rate is proportional to T^2, while electron-phonon scattering rate is proportional to T^5 [31]. The conductivity increase on a time scale of the electron-phonon interaction can be assigned to the fact that the drop in the electronic temperature is substantially larger than the increase in the phonon temperature. After the temperatures of the electrons and the lattice are equilibrated, the whole excited area will cool down on the time scale of the heat transfer ($\tau_2 \sim 140$ ps). Therefore, τ_2 is assigned to the cooling of the lattice, which results in the coupling of the lattice to an infinite reservoir at room temperature and is not explicitly shown in this restricted two-temperature model. As the electron scattering decreases (due to electron-phonon coupling and heat transfer) the conductivity increases and thus the THz transmission decreases, this behavior is consistent with Fig. 2.

In Fig. 3(b) we show τ_1 and τ_2 as function of temperature, τ_0 appears to be temperature-independent $\tau_0 \sim 0.16$ ps. The fast recovery (τ_1) on a subpicosecond time scale is nearly independent of the sample temperature, whereas the slow cooling rate (τ_2) increases by almost 15% when going from 300 to 15 K. Since τ_2 corresponds to the characteristic time

of the longer thermal relaxation process, as the temperature increases, the thermal relaxation is more efficient and τ_2 decreases. On the other hand, τ_1 (which is related to the electron-phonon coupling) is independent on the temperature since it is mainly affected by the ultrafast heating caused by the optical laser pulse. As for the exponential decay amplitudes of the transmission (A_1 and A_2) a decrease is observed for increasing temperatures [Fig. 3(c)]. This result is expectable since, for high temperatures, the transmission limit is enhanced and thus the decay amplitudes decrease.

Measurements with different in-plane magnetic fields were also performed (not shown). For the best sensitivity of our setup we could not detect any dependence of the THz transmission, with or without pump, on the magnetic field. This is probably related with the small magnetoresistance exhibited in this sample [24]. Furthermore, while magnetoresistive effects are claimed to be abundantly observed in the midinfrared optical range [32–36], less is known for the THz spectral range [37–39].

To understand the effect of light on the $CoFe/Al_2O_3$ multilayer structure we also studied THz emission from the sample after it has been excited by a femtosecond laser pulse at room temperature. Figure 4(a) shows the THz emission waveforms measured at different azimuthal angles (θ) between magnetization and the axis of the electrooptical detector (polarization of the detection beam). The polarization of the detection beam was maintained constant and the sample rotated. To elucidate the origin of the emission, we have performed the measurements for different orientations of the magnetization with respect to the axis of the detector. Although we clearly observe THz emission when the polarization of the detector axis and the magnetization are orthogonal, no THz emission is observed with the axis parallel to the magnetization. To reveal the full angular dependence we have measured the strength of the electric field of the emitted THz radiation as a function of the angle θ between the detector axis and the magnetization. Figure 4(b) reveals a periodic dependence that can be accurately fit with a sine function. A similar sinusoidal relation to the laser-induced THz emission was already observed in Fe [40] and Ni films [14]. While the former report claimed that this emission is generated by an optical nonlinearity due to symmetry breaking at the surfaces of the films, the latter suggested that the THz emission originates from the ultrafast laser-induced demagnetization of the metallic magnet. Indeed, it follows from Maxwells's equations that a time varying magnetization (M) results in the emission of electromagnetic radiation.

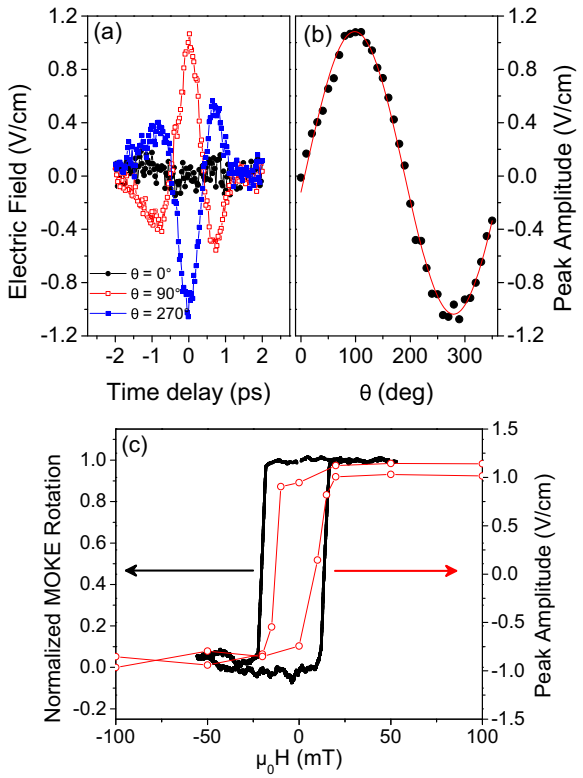

FIG. 4. (Color online) Ultrafast demagnetization results in THz emission. (a) THz emission for different azimuthal angles θ. (b) Experimental peak intensity as a function of θ (dots) and respective sinusoidal fit (line). (c) Comparison between the near-infrared MOKE rotation and the THz peak amplitude as a function of the applied magnetic field.

To confirm that the origin of the THz emission is the ultrafast demagnetization, we performed experiments at different applied magnetic fields (H). Since CoFe is a ferromagnetic material, the dependence of the magnetization M on the field H shows a hysteretic behavior. Using magnetooptical Kerr effect (MOKE) measurements [41] in which the angle of incidence of light was set to 45° and the magnetic field applied in the plane of the sample, we obtained the dependence of the magnetization on the magnetic field $M(H)$ [see Fig. 4(c)]. The figure also shows that the peak amplitude of the emitted THz radiation as a function of H reveals a similar hysteresic-like behavior. It should be noted, however, that since the THz emission measurements run in a stroboscopic mode with pump pulses present, the interpretation of the outcome of the measurements in fields lower than the coercive field is ambiguous.

We have also checked if the THz emission is sensitive to the polarization of the optical pump and found no polarization dependence of the emission signals which again confirms the hypothesis that the ultrafast changes of the magnetization are due to the laser-induced demagnetization and not optomagnetic phenomena similar to those described in Ref. [42]. It was observed (using wiregrid polarizers) that the emission is always purely polarized perpendicular to the magnetization. These measurements support the hypothesis that demagnetization induced THz emission is observed.

To support the idea of THz radiation being emitted due to ultrafast laser-induced demagnetization, we have compared our experimental results obtained with the help of the MOKE and THz emission spectroscopy. In particular, taking the data on ultrafast demagnetization from the MOKE measurements we calculated the electric field of the THz wave emitted as a result of such a rapid change of the magnetization of the medium. Starting from the derivation of the plane wave equation for an infinite plane, using Faraday's and Ampère's laws and taking into account the fact that the generated THz radiation before being detected first propagates through a glass substrate, we come to the following expression for the electric

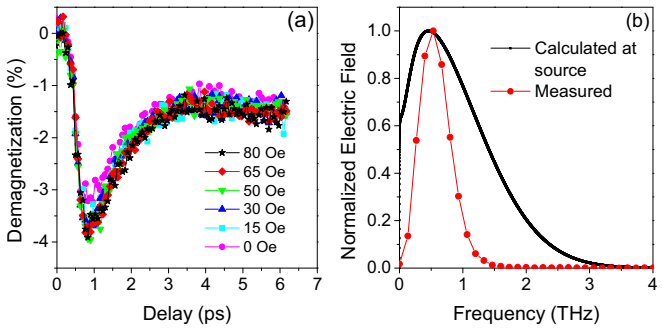

FIG. 5. (Color online) Ultrafast demagnetization results in a near-infrared pump-probe system. (a) Pump-probe measurements of the demagnetization at different applied magnetic fields and (b) comparison between the spectrum of the THz emission and the spectrum calculated through the demagnetization measurements (both normalized to their highest value).

field of the THz radiation:

$$\tilde{E}_y(\omega,z) = \frac{4\pi\omega}{c} i\tilde{m}_x(\omega) d \frac{1}{n+1} \exp\left(-i\frac{\omega}{c} nz\right), \qquad (4)$$

where $\tilde{E}_y(w,z)$ is the generated complex electric field, $\tilde{m}_x$ is the complex magnetization, ω the angular frequency, d is the thickness of the magnetic layer, n is the refractive index of the substrate, and c the speed of light in a vacuum. A detailed description of these calculations is reported elsewhere [43].

To find the electric field of the generated THz radiation, we experimentally found how the magnetization of the medium changes in time after the sample was excited by a 50-fs laser pulse at room temperature. In particular, we performed all optical pump-probe experiments in which the medium was excited by a 50-fs laser pulse with a central wavelength of 800 nm and the temporal evolution of the laser-induced changes was probed with the help of a similar, but weaker probe pulse. Using the procedure described in Ref. [44], we were able to determine the time scale and the degree of the laser-induced demagnetization [Fig. 5(a)]. The dynamics of the demagnetization obtained at different magnetic fields are shown in Fig. 5(a), revealing that it is relatively insensitive to the external magnetic field.

Taking the dependence of the demagnetization from Fig. 5(a) we calculated the spectrum of the THz emission. The outcome of the calculations is shown in Fig. 5(b), together with the measured trace of the THz spectrum. Regarding the fact that in the calculation procedure of the THz trace no fit parameters are used and the propagation and ZnTe response are neglected, the similarity between these two spectra is quite satisfactory. However, the spectral width of the calculated spectrum is broader than the measured one. This can be explained by taking into account that the propagation response will attenuate lower frequencies, while the propagation through the substrate and the response of the ZnTe detection will attenuate higher frequencies.

In summary, a detailed study of the THz transmission and emission in CoFe/Al_2O_3 multilayers was performed. It was verified that the THz transmission has the same temperature dependence as the electrical resistance, opening the possibility of studying spintronic phenomena in the THz spectral range. Moreover, the effect of a femtosecond laser excitation on the THz transmission, and thus the electrical resistivity, was studied. Besides the observed subpicosecond change in the resistivity, we also observed an emission of linearly polarized THz radiation triggered by the ultrafast optical excitation. To reveal the origin of the emission, we compared the near-infrared MOKE rotation with the THz peak amplitude. Both these observables appear to show quite similar hysteresis dependencies on the applied magnetic field. Moreover, the magnetization dynamics deduced from the time-resolved MOKE measurements was used to calculate the spectrum of the THz emission which must accompany such a laser-induced magnetization dynamics. The calculated spectrum is in quite good agreement with the experimentally obtained spectrum of the electric field of the emitted radiation. These facts strongly support the hypothesis that the THz emission originates from the ultrafast laser-induced demagnetization.

This work was supported by the 7th Framework Program (EU-FP7) Grant No. NMP-3-LA-2010-246102 (IFOX Project), European Research Council ERC Grant No. N257280 (femtomagnetism), Projects No. Norte-070124-FEDER-000070, FEDER-POCTI/0155, No. PTDC/CTMNAN/112672/2009, No. PTDC/CTM-MET/118236/2010, and No. PTDC/FIS/120055/2010. Funding from the Foundation for Fundamental Research on Matter (FOM) and from FCT through the Associated Laboratory-IN is acknowledged. J.M.T. and J.D.C. are thankful for FCT Grants (No. SFRH/BPD/72329/2010 and No. SFRH/BD/79393/2011, respectively). J.V. and G.N.K. acknowledge the financial support of FSE/POPH.

[1] I. Zutic, J. Fabian, and S. Das Sarma, Rev. Mod. Phys. **76**, 323 (2004).
[2] A. Kirilyuk, A. V. Kimel, and T. Rasing, Rev. Mod. Phys. **82**, 2731 (2010).
[3] E. Beaurepaire, J.-C. Merle, A. Daunois, and J.-Y. Bigot, Phys. Rev. Lett. **76**, 4250 (1996).
[4] A. V. Kimel, A. Kirilyuk, P. A. Usachev, R. V. Pisarev, A. M. Balbashov, and Th. Rasing, Nature (London) **435**, 655 (2005).
[5] C. D. Stanciu, F. Hansteen, A. V. Kimel, A. Kirilyuk, A. Tsukamoto, A. Itoh, and Th. Rasing, Phys. Rev. Lett. **99**, 047601 (2007).
[6] R. Ulbricht, E. Hendry, J. Shan, T. F. Heinz, and M. Bonn, Rev. Mod. Phys. **83**, 543 (2011).
[7] M. A. Ordal, Robert J. Bell, R. W. Alexander, Jr., L. L. Long, and M. R. Querry, Appl. Opt. **24**, 4493 (1985).
[8] M. C. Beard, G. M. Turner, and C. A. Schmuttenmaer, Phys. Rev. B **62**, 15764 (2000).

[9] E. Hendry, F. Wang, J. Shan, T. F. Heinz, and M. Bonn, Phys. Rev. B **69**, 081101 (2004).

[10] E. Hendry, M. Koeberg, J. Pijpers, and M. Bonn, Phys. Rev. B **75**, 233202 (2007).

[11] S. W. Koch, M. Kira, G. Khitrova, and H. M. Gibbs, Nat. Mater. **5**, 523 (2006).

[12] M. van Exter and D. Grischkowsky, Phys. Rev. B **41**, 12140 (1990).

[13] T. Jeon and D. Grischkowsky, Appl. Phys. Lett. **72**, 3032 (1998).

[14] E. Beaurepaire, G. M. Turner, S. M. Harrel, M. C. Beard, J.-Y. Bigot, and C. A. Schmuttenmaer, Appl. Phys. Lett. **84**, 3465 (2004).

[15] J. Shen, H.-W. Zhang, and Y.-X. Li, Chin. Phys. Lett. **29**, 067502 (2012).

[16] R. V. Mikhaylovskiy, E. Hendry, F. Y. Ogrin, and V. V. Kruglyak, Phys. Rev. B **87**, 094414 (2013).

[17] K. Mori, T. Satoh, R. Iida, T. Shimura, and K. Kuroda, in QEC/CLEO Pacific Rim, *Proceeding of Quantum Electronics Conference Lasers and Electro-Optics* QEC/CLEO Pacific Rim (IEEE, New York, 2011).

[18] K. Yamaguchi, M. Nakajima, and T. Suemoto, Phys. Rev. Lett. **105**, 237201 (2010).

[19] K. Yamaguchi, T. Kurihara, Y. Minami, M. Nakajima, and T. Suemoto, Phys. Rev. Lett. **110**, 137204 (2013).

[20] T. Kampfrath, M. Battiato, P. Maldonado, G. Eilers, J. Nötzold, S. Mährlein, V. Zbarsky, F. Freimuth, Y. Mokrousov, S. Blügel, M. Wolf, I. Radu, P. M. Oppeneer and M. Münzenberg, Nat. Nanotech. **8**, 256 (2013).

[21] J. Kono, Nat. Photon. **5**, 5 (2011).

[22] J. S. Moodera, Lisa R. Kinder, Terrilyn M. Wong, and R. Meservey, Phys. Rev. Lett. **74**, 3273 (1995).

[23] J. Ventura, A. M. Pereira, J. P. Araujo, J. B. Sousa, Z. Zhang, Y. Liu, and P. P. Freitas, J. Phys. D: Appl. Phys. **40**, 5819 (2007).

[24] J. B. Sousa, J. A. M. Santos, R. F. A. Silva, J. M. Teixeira, J. Ventura, J. P. Araujo, P. P. Freitas, S. Cardoso, Yu. G. Pogorelov, G. N. Kakazei, and E. Snoeck, J. Appl. Phys. **96**, 3861 (2004).

[25] W. Kleemann, O. Petracic, Ch. Binek, G. N. Kakazei, Yu. G. Pogorelov, J. B. Sousa, S. Cardoso, and P. P. Freitas, Phys. Rev. B **63**, 134423 (2001).

[26] G. N. Kakazei, P. P. Freitas, S. Cardoso, A. M. L. Lopes, M. M. Pereira de Azevedo, Yu. G. Pogorelov, and J. B. Sousa, IEEE Trans. Magn. **35**, 2895 (1999).

[27] K. Reimann, Rep. Prog. Phys. **70**, 1597 (2007).

[28] J. K. Chen and J. E. Beraun, Numer. Heat Transfer A **40**, 1 (2001).

[29] B. Hillebrands and K. Ounadjela, *Spin Dynamics in Confined Magnetic Structures I* (Springer, New York, 2002).

[30] A. Ellens, H. Andres, A. Meijerink, and G. Blasse, Phys. Rev. B **55**, 173 (1997).

[31] J. M. Ziman, *Electrons and Phonons, The Theory of Transport Phenomena in Solids* (Oxford University Press, New York, 1960).

[32] J. C. Jacquet and T. Valet, Mater. Res. Soc. Symp. Proc. **384**, 477 (1995).

[33] S. Uran, M. Grimsditch, Eric E. Fullerton, and S. D. Bader, Phys. Rev. B **57**, 2705 (1998).

[34] A. B. Granovsky, I. V. Bykov, E. A. Gan'shina, V. S. Gushchin, M. Inoue, Yu. E. Kalinin, A. A. Kozlov, and A. N. Yurasov, J. Exp. Theor. Phys. **96**, 1104 (2003).

[35] R. F. C. Marques, P. R. Abernethy, J. A. D. Matthew, C. O. Paiva-Santos, L. Perazolli, M. Jafelicci, Jr., and S. M. Thompson, J. Magn. Magn. Mater. **272-276**, 1740 (2004).

[36] R. T. Mennicke, D. Bozec, V. G. Kravets, M. Vopsaroiu, J. A. D. Matthew, and S. M. Thompson, J. Magn. Magn. Mater. **303**, 92 (2006).

[37] R. Shimano, Y. Ino, Yu. P. Svirko, and M. Kuwata-Gonokami, Appl. Phys. Lett. **81**, 199 (2002).

[38] K. J. Chau and A. Y. Elezzabi, Phys. Rev. Lett. **96**, 033903 (2006).

[39] C. J. E. Straatsma, M. Johnson, and A. Y. Elezzabi, J. Appl. Phys. **112**, 103904 (2012).

[40] D. J. Hilton, R. D. Averitt, C. A. Meserole, G. L. Fisher, D. J. Funk, J. D. Thompson, and A. J. Taylor, Opt. Lett. **29**, 1805 (2004).

[41] J. M. Teixeira, R. Lusche, J. Ventura, R. Fermento, F. Carpinteiro, J. P. Araujo, J. B. Sousa, S. Cardoso, and P. P. Freitas, Rev. Sci. Instrum. **82**, 043902 (2011).

[42] A. V. Kimel, A. Kirilyuk, and T. Rasing, Laser Photon. Rev. **1**, 275 (2007).

[43] T. J. Huisman, R. V. Mikhaylovskiy, A. Tsukamoto, Th. Rasing, and A. V. Kimel, arXiv:1412.5396.

[44] R. Medapalli, I. Razdolski, M. Savoini, A. R. Khorsand, A. Kirilyuk, A. V. Kimel, Th. Rasing, A. M. Kalashnikova, A. Tsukamoto, and A. Itoh, Phys. Rev. B **86**, 054442 (2012).